REVIEW
High speed fusion weld bead defects

T. C. Nguyen[1], D. C. Weckman*[2], D. A. Johnson[2] and H. W. Kerr[2]

A comprehensive survey of high speed weld bead defects is presented with strong emphasis on the formation of humping and undercutting in autogenous and non-autogenous fusion welding processes. Blowhole and overlap weld defects are also discussed. Although experimental results from previous studies are informative, they do not always reveal the physical mechanisms responsible for the formation of these high speed weld bead defects. In addition, these experimental results do not reveal the complex relationships between welding process parameters and the onset of high speed weld bead defects. Various phenomenological models of humping and undercutting have been proposed that were based on observations of events in different regions within the weld pool or the final weld bead profile. The ability of these models to predict the onset of humping or undercutting has not been satisfactorily demonstrated. Furthermore, the proposed formation mechanisms of these high speed weld bead defects are still being questioned. Recent welding techniques and processes have, however, been shown to be very effective in suppressing humping and undercutting by slowing the backward flow of molten metal in the weld pool. This backward flow of molten weld metal may be the principal physical phenomenon responsible for the formation of humping and undercutting during high speed fusion welding.

Keywords: High speed weld bead defects, Humping

Introduction

To remain competitive in today's manufacturing environment, companies must continuously improve their productivity without sacrificing the quality of their products. Increases in productivity will reduce overall production costs thereby maintaining and strengthening the company's competitiveness. Since welding is ubiquitous and an integral part of most manufacturing industries such as the construction, shipbuilding, aerospace, automotive, petrochemical and electronic industries, overall production costs can usually be reduced by evaluating the productivity of the welding processes used.

There are a number of general approaches that can be used to improve the productivity of a particular welding operation. The existing welding process can be optimised in order to maximise welding speeds. Further gains in productivity, repeatability and weld quality may be realised by automating the welding process. Finally, selecting and implementing newer welding processes that are intrinsically capable of much greater welding speeds than is possible with the existing welding processes may help to realise significant gains in productivity. In addition to productivity increases, high welding speeds can also have other benefits such as improved melting efficiency and lower distortion, because as welding speed is increased, most of the incident heat contributes to forming the weld and less is lost by conduction into the surrounding weldment.[1,2]

All fusion welding processes are multivariate, frequently with synergistic, nonlinear interactions between the numerous process variables. Therefore, increased productivity in a fusion welding process cannot be realised simply by increasing the welding speed without affecting other welding parameters. Some insights into these interactions are possible through consideration of Rosenthal's[3] analytical models for heat conduction in fusion welds made in thick or thin plates using point or line heat sources respectively. For example, working from Rosenthal's models,[3] Adams[4] has shown that the cooling rate down the centre line of the weld and the width of the heat affected zone (HAZ) are proportional to the heat input per unit distance of weld H_{net} (J m^{-1}), as given by

$$H_{net} = \frac{\eta\, Q}{v_w} \qquad (1)$$

where η is the arc efficiency; Q (W) is the power generated by the heat source and v_w (m s^{-1}) is the welding speed.[4] From equation (1), it should be possible to increase welding speed and productivity while maintaining the same cooling rate or HAZ size provided that H_{net} is maintained constant, i.e. Q must be increased at the same rate as v_w.

The theoretical predictions embodied in equation (1) suggest that unbounded increases in productivity are possible by simply increasing Q at the same rate as v_w. In

[1]School of Engineering and Information Technology, Conestoga College, 299 Doon Valley Dr., Kitchener, Ontario N2G 4M4, Canada
[2]Department of Mechanical Engineering, University of Waterloo, Waterloo, Ontario N2L 3G1, Canada

*Corresponding author, email dweckman@uwaterloo.ca
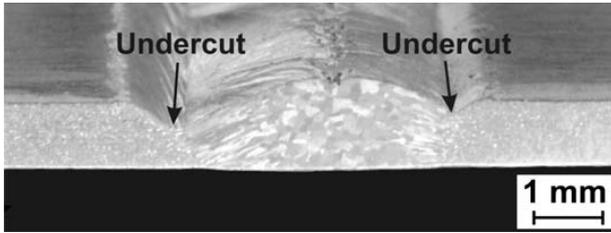
1 Top weld bead and transverse section of high speed variable polarity plasma arc weld made in AA5182 aluminium alloy sheet exhibiting severe undercut

practice, however, the welding speed will be limited by the deterioration of the weld bead quality as welds begin to exhibit serious geometric defects such as undercutting and humping.[5,6] Located in the weld metal adjacent to the weld toe, undercut is a sharp groove left unfilled by the weld metal during solidification.[6] An example of a weld with severe undercutting is shown in Fig. 1. Undercut creates a mechanical notch at the weld interface that lowers the static, fatigue and fracture strength of the welded assembly. In certain advanced manufacturing applications such as tailor welded blanks, undercut will also reduce the formability of the blank.[7]

Humping can be described as a periodic undulation of the weld bead. An example of humping in a bead on plate gas metal arc (GMA) weld made in mild steel is shown in Fig. 2a.[8,9] Transverse sections of this weld at a valley (section a-a) and a hump (section b-b) are shown in Fig. 2b and c respectively. At both the valley and the hump, the depth of penetration is the same. However, there is a large accumulation of weld metal at the hump. The overall appearance of a humped weld suggests that its formation is a periodic physical phenomenon in an otherwise steady welding process.

The undercut and humping weld defects produced at high welding speeds will compromise the mechanical integrity of the joint, thereby imposing an upper limit to the welding speed and overall production rates. To achieve further gains in productivity, the formation of these high speed weld defects must be eliminated or suppressed to higher welding speeds. This requires a thorough understanding of the physical phenomena responsible for the formation of these weld defects.

In the present article, a review of the current literature related to high speed weld bead defects for different fusion welding processes will be presented. The review will concentrate mostly on humping and undercutting weld defects; however, blowhole and overlap defects in welds will also be briefly discussed. The present article will be divided into three sections. First, parametric studies of the effects of various welding parameters on the formation of these weld defects will be discussed. Second, the different phenomenological models that have been proposed to explain the physical phenomena responsible for the development of these defects will be examined. Last, welding techniques and processes that are currently known to be capable of suppressing or eliminating these high speed weld defects thereby facilitating higher welding speeds and increased productivity will be reviewed.
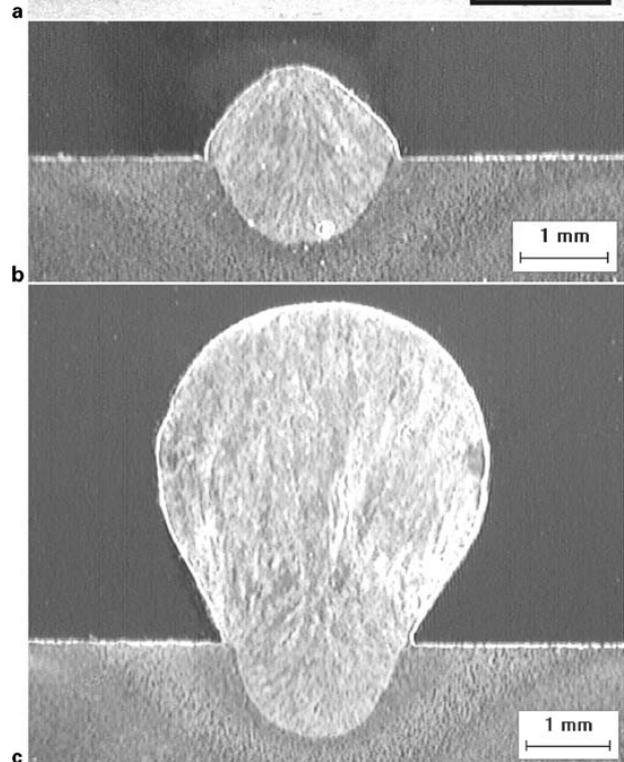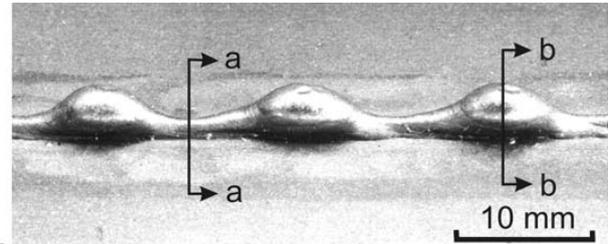
a humped weld bead; *b* transverse section at a-a; *c* transverse section at b-b (taken from Nguyen et al.[8,9])

2 Humping in bead on plate GMA weld made on cold rolled AISI 1020 plain carbon steel

Effects of weld process parameters on high speed welding defects

Over the years, as welding processes have been automated and greater welding speeds were made possible, welders have become increasingly aware of the occurrence of humping and undercutting at higher welding speeds. To eliminate these weld defects, a slower welding speed is often recommended. This option, however, is contrary to the continuous pressures for ever increasing welding speeds and productivity.

Because fusion welding processes have many parameters, frequently with multiple, nonlinear interactions, it should not be surprising that welding speed is not the only weld process parameter that influences undercut and humping defect formation.[5,8,9] Clearly, the first step towards developing a comprehensive understanding of the undercut and humping phenomena in any welding process is the determination through experiments of all welding parameters that affect these defects. Performing welding experiments designed to map the range of these parameters that will produce welds with the undercut and humping defects and identification of process parameter interactions will then provide better understanding of the effects of process parameters on the occurrence of these defects.
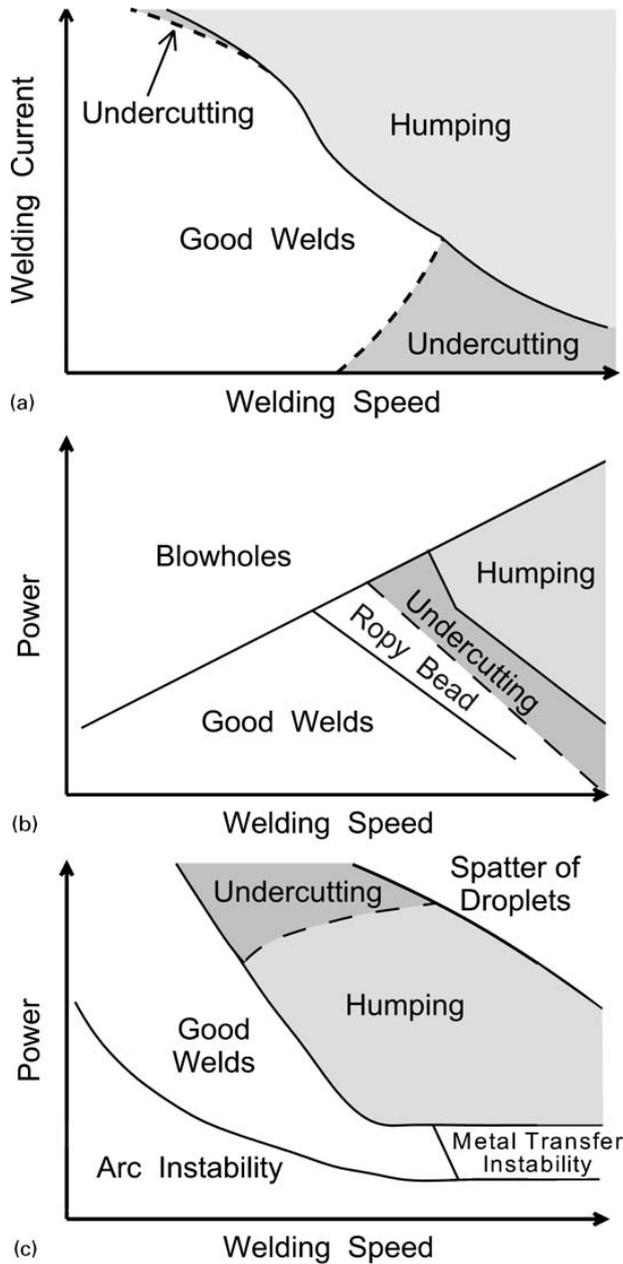
a GTAW of plain carbon steel after Savage *et al.*;[12]
b CO_2 laser welding of 304 stainless steel after Albright and Chiang;[14] *c* GMAW of mild steel after Nishiguchi *et al.*[10]

3 Mapping of various weld bead regions

Humping and undercutting are found in both non-autogenous (filler metal added) welding processes such as gas metal arc welding (GMAW) and submerged arc welding (SAW)[5,8–10] and autogenous (no filler metal) processes such as gas tungsten arc welding (GTAW),[11,12] laser beam welding (LBW)[13,14] and electron beam welding (EBW).[15–17] The formation of humps and undercuts when using these welding processes have been attributed to the effects of various process parameters such as welding speed, power input, surface condition of the work piece, base metal chemical composition, the electrode geometry, the type and composition of shielding gas used, the travel angle of the heat source and the orientation of the work piece with respect to gravity, i.e. whether welding is in the flat position, uphill or downhill.[5,8,9,11] Often, systematic mapping of various

weld bead profiles observed versus the relevant weld process parameters has been performed.[8–12,14–16] In Fig. 3, for example, the influences of welding speed, welding current or power input on the formation of humping and undercutting in autogenous GTAW of a precipitation hardenable steel[12] (Fig. 3*a*), in autogenous CO_2 LBW of thin 304 stainless steel sheets[14] (Fig. 3*b*) and in non-autogenous GMAW of mild steel plate[10] (Fig. 3*c*) are shown. Although the fusion welding processes and their controlling parameters used to generate the process maps shown in Fig. 3*a*–*c* are fundamentally different, there are common trends in behaviour. In all cases, the welding speed limit is defined by the occurrence of undercuts at low powers and humps at medium power input levels.[11,12,16] At high power input levels, the welding speed is restricted by a combination of humped welds and severe undercuts.[5,11,14,15] Finally, there appears to be an inverse relationship between the welding speed limit and total power, i.e. the welding speed limit decreases as the total power increases.

The presence of severe undercutting at high power input levels is not always observed. Nishiguchi *et al.*[10] and Tsukamoto *et al.*[16] reported that humped welds without undercut were observed at high power input levels in GMAW and EBW respectively. In contrast, Bradstreet[5] and Hiramoto *et al.*[13] reported humping with undercutting in high power GMAW and EBW respectively. Interestingly, Hiramoto *et al.*[13] also observed humping without undercutting in LBW.

A comparison between the GMAW experimental procedures used by Bradstreet,[5] Nguyen *et al.*[8,9] and Nishiguchi *et al.*[10] reveals that different modes of filler metal transfer were used in their respective studies. Nishiguchi *et al.*[10] employed short circuit and globular transfer modes while Bradstreet[5] and Nguyen *et al.*[8,9] used spray transfer mode. Furthermore, Nishiguchi *et al.*[10] employed the buried arc technique to minimise the amount of weld spatter. Therefore, the lack of undercut may be related to the different metal transfer modes of GMAW and the effects of burying the welding arc. The observed difference indicates that the welding technique and the metal transfer mode in GMAW influence the weld bead geometry. The interactions between metal transfer mode and the occurrence of humping and undercutting further complicate welding process maps such as that shown in Fig. 3*c*. These interactions are not yet clearly understood.

The influences of a number of other process variables on the formation of undercutting and humping have also been reported. Yamauchi and Taka[18,19] and Savage *et al.*[12] showed that GTAW speeds could be more than doubled when He was used instead of Ar as shielding gas. The beneficial effects of using lower molecular weight of He shielding gas was attributed to the influences of arc forces on depression of the weld pool under the arc Savage *et al.*[12] found that there was no measurable difference between total arc force when using either Ar or He and concluded that the observed effects must be due to lower peak arc pressures and the characteristic increased width of He arcs. These conclusions were verified by arc pressure measurements made by Yamauchi and Taka.[18,19] They found that the peak arc pressure of He arcs was significantly lower than Ar arcs under the same welding conditions.

The ambient pressure also has been shown to have an effect on the humping phenomenon. Nishiguchi and Matsunawa[20] made GMA welds on plain carbon steel in a hyperbaric chamber at Ar atmosphere pressures up to five bars and found that the critical welding speed above which high speed defects such as humping occurred increased with increased hyperbaric pressures. They noted that the arc and oxide cleaning by the arc became more focused with increased ambient pressure and that the weld pool profile changed from the normal nail head profile commonly observed with spray transfer to a semicircular profile with increased penetration. Unfortunately, the increased costs and welding times associated with hyperbaric welding would be prohibitive in most production situations.

The use of reactive shielding gases such as CO_2 and Ar–CO_2 or Ar–O_2 mixes[5,8,9,21] as well as trimixes such as Ar–CO_2–O_2[21] and quad mixes such as Ar–CO_2–O_2–He[8,9] in GMAW and He shielding gas in GTAW[11] have been found to expand the range of operating conditions in which good welds are produced to as much as 400% higher welding speeds relative to welds produced using Ar shielding gas.[8,9] Bradstreet[5] and Nguyen et al.[8,9] noted that the contact angle between the molten metal and the fusion boundary of GMA welds in mild steel was reduced and wetting between the weld metal and base metal improved when even a small percentage (2–5%) of oxygen was added to the Ar shielding gas. Because an interfacial surface tension force balance exists at the point of contact between the liquid metal and the solid fusion boundary,[5] this reduced contact angle is direct evidence that the liquid metal surface tension has been reduced by the addition of O_2, possibly through formation of SiO_2 or FeO oxide films on the surface of the molten steel. In fact, Subramaniam and White[22] have made in situ measurements of the surface tension of molten metal droplets in a GMAW plasma and found that the surface tension of the molten metal in the plasma is decreased from $\sim 1 \cdot 56$ to $\sim 1 \cdot 1$ N m^{-1} when O_2 or CO_2 is added to the Ar shielding gas.

When using reactive shielding gases, the resultant lower values of liquid metal surface tension influence the initial contact angle between the molten weld metal and the surface of the work piece.[5] Bradstreet[5] argued that this change in the initial contact angle delays the onset of humping. This is further supported by an analogue study of bead geometry stability by Schiaffino and Sonin,[23] in which a fine stream of microcrystalline wax droplets was projected onto the surface of a moving plate of Plexiglass. They also found that the contact angle between the molten wax and the surface of the Plexiglass work piece was responsible for the instability of the wax bead geometry. When this angle was $<\pi/2$ radians (90°), humping would not occur. On the other hand, if the initial contact angle was $>\pi/2$ radians (90°), the wax bead was unstable and formed periodic undulations similar to the humping phenomenon in welding. Schiaffino and Sonin[23] suggested that the initial contact angle is a function of the liquid's properties and is also strongly dependent on the temperature difference between the initial temperature of the work piece and the melting temperature of the deposited liquid.

In GTAW, the electrode geometry has also been shown to suppress the onset of humping and undercutting to higher welding speeds. Use of larger electrode tip angles or smaller electrode diameters is reported to be beneficial to achieving higher welding speeds during GTAW.[11,18] Yamauchi and Taka[19] have also shown that significantly higher welding speeds are possible when hollow electrodes are used. Similarly, Nishiguchi et al.[10] have found that use of a larger electrode wire during GMAW will suppress the creation of high speed weld defects in GMA welds. All of these electrode geometry effects are known to reduce arc forces and the amount of depression of the weld pool surface directly under the welding arc.[18,19,24] Arc forces are created by momentum transfer that takes place when the high velocity stream of plasma in the welding arc impinges on the weld pool surface. The plasma within the arc is driven down from the electrode to the weld pool surface by the difference in Lorentz force $\vec{F}_{L} = \vec{J} \times \vec{B}$, between the electrode and the weld surface as well as the axial component of the Lorentz force where $\vec{J}$ is the current density and $\vec{B}$ is the magnetic field vector. As the electrode tip angle increases, for example, the arc changes from a bell shape with a large difference in $\vec{J}$ at the electrode relative to $\vec{J}$ at the weld surface to a more column like arc with less difference between $\vec{J}$ along the length of the arc and, therefore, less driving force for flow of the plasma. Therefore, any electrode geometry such as a hollow electrode or larger electrode tip angle that produces a more column like arc will result in lower plasma velocities, lower arc forces and, therefore, less depression of the weld pool surface and decreased propensity for humping and undercutting.[18,19,24] While electric arcs and arc forces are not present in high energy density processes such as EBW and LBW, lowering the energy density of the heat source at the work piece surface[13] or over focusing[15] have been shown to facilitate production of defect free welds at higher welding speeds, because there is less depression of the weld pool surface owing to vaporisation.

Regardless of the type of heat source, the travel angle between the heat source and welding direction has been found to affect the onset of undercut and humping. Use of a positive push angle of the heat source or forehand welding has been shown to suppress the formation of the undercut and humping defects to higher welding speeds.[5,11,25] This is thought to occur because the heat source is impinging more directly on unmelted base metal and is less able to depress the surface of the weld pool, whereas, use of a trailing heat source angle results in greater depression of the weld pool surface and active pushing of the molten metal towards the tail of the weld pool, thereby promoting humping at lower welding speeds and powers.[5,8,9]

Nguyen et al.[8,9] have shown that the orientation of the work piece with respect to gravity also affects the propensity for humping during GMAW. They found that welding could be performed at higher speeds without humping when welding downhill, because gravitational forces weaken the backward flow of molten metal in the weld pool and the molten metal tends to flow down from the tail of the weld back into the weld pool. Alternatively, welding in the uphill direction promoted humping at lower speeds, because gravitational forces further strengthen the backward flow of molten metal and push the molten metal towards the tail of the weld pool thereby promoting humping.
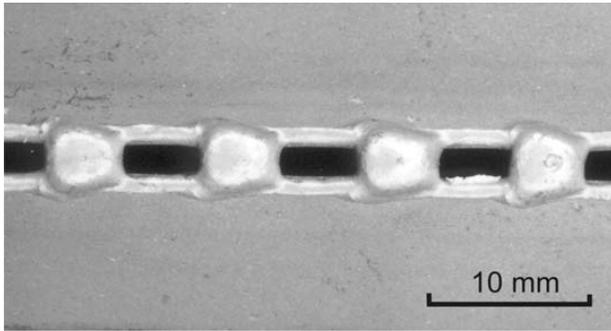
4 **Severe blowhole defects in semiautomated GTA weld made in 16 gauge mild steel sheets in corner joint configuration (taken from Biglou[33])**

Besides undercutting and humping, two other types of high speed weld defects have been reported: through thickness holes or blowholes in full penetration LBW and EBW welds in thin sheets[14,25–28] and overlap defects in high speed welding of stainless steels.[15,25,26,29–32] An example of through thickness hole or blowhole defect in semiautomated GTAW of 16 gauge mild steel sheets is shown in Fig. 4.[33] The weld bead of welds exhibiting through thickness hole or blowhole defects is broken up by regularly or irregularly spaced holes.[14,33] According to Albright and Chiang,[14] the occurrences of through thickness holes are generally an indication of excessively high levels of heat input per unit distance (see Fig. 3b) which results in full penetration welds with excessive weld widths relative to the sheet thickness. These wide welds are subject to blow through defects owing to the combined effects of arc forces and gravity and are also affected by capillary instabilities similar to the Rayleigh instability model used by Bradstreet[5] to explain humping in GMAW.

If the welding speed is further increased, the overlap defect may begin to form.[6,15,17] Figure 5 is a schematic of the top view and the transverse section of an overlap defect in a weld produced using high power input and welding speed. The overlap defect is formed when the molten metal overflows the weld pool and solidifies on the top surface of the work piece without fusing to the base metal. This creates an incipient crack between the over flowed weld metal and the base metal. The weld bead can also exhibit a deep groove along the centre of the bead. Under certain extreme welding conditions, overlaps have been observed to form two parallel humped beads along the adjacent fusion boundaries of the weld.[29–32] These overlap defects have been reported most frequently to occur in austenitic stainless steel welds when using the EBW[15,26] or the GTAW[25,29–32] processes, but were also observed by Bradstreet[5] during GMAW of mild steel.

There are two proposed explanations for the formation of the overlap defect. Tomie *et al.*[17] speculated that at higher EBW speeds, molten weld metal from the front of the weld pool could not easily flow back to the tail of the weld pool owing to an enlarged beam cavity and smaller weld pool width. The inclined front wall of the weld pool at high welding speed also caused molten weld metal to flow out of the weld pool as it went around the beam cavity to form the overlap on the top surface of the work piece.[17,26] On the other hand, it has been suggested that for low energy density welding processes
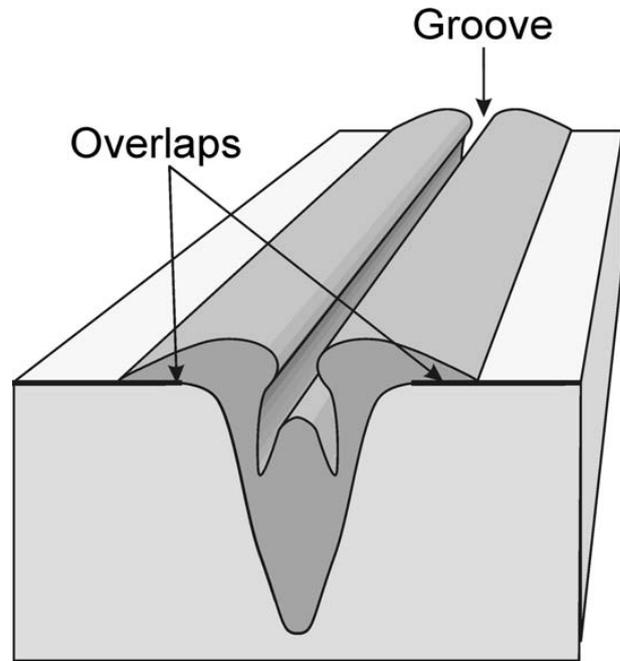
5 **Schematic drawing illustrating cross-section and top view of overlap defect in autogenous weld produced at high welding power and welding speed**

such as GTAW, the overlaps form as the molten weld metal is split into two streams around the welding arc while being displaced from the front to the rear of the weld pool.[29–32] According to Brooks and Lippold,[34] molten austenitic stainless steel is highly viscous and sluggish compared to other grades of stainless steel. The high viscosity reduces the flow and the wettability of molten weld metal thereby preventing merging of the two streams behind the welding arc prior to solidification of the liquid metal. At high welding speeds, these two streams of molten metal may solidify individually on the cooler edges of the weld pool, thereby causing the overlap defect.

While empirical plots such as those shown in Fig. 3 are very informative, they are somewhat limited because they do not show the effects of all influential process parameters. In each plot, the effects of various combinations of welding speed and power input are evident while other process parameters were kept constant. A minor change in one of the other process variables such as selecting a different shielding gas composition can significantly displace the boundaries of the weld profile regions.[8–11] Therefore, a new plot is needed to properly illustrate the effect of a minor change in one variable. This is time consuming and costly as many experimental welds are required to generate these process maps.

Table 1 contains a summary of the welding processes, materials, weld types and process parameters that have been examined by different researchers. In general, most studies have used bead on plate welding to explore the influence of welding speed and welding power on the undercut and humping phenomena. However, it is clear from the experimental results discussed above and in Table 1 that there are a number of other welding process parameters that affect the undercut and humping phenomena and that there are frequently nonlinear interactions between all of these parameters. In general,

Table 1 Welding process parameters that have been examined in studies of undercutting and humping as well as various proposed models used to explain formation of these high speed weld defects

Year	1968	1971	1975	1975	1978	1978, 1979	1979	1982	1982, 1983	1987	1988	1989	1990	1992	2002	1998–2003	2005
Authors	Bradstreet	Paton et al.	Nishiguchi et al.	Yamamoto et al.	Arata et al.	Yamauchi and Taka	Savage et al.	Shimada et al.	Tsukamoto et al.	Hiramoto et al.	Albright and Chiang	Tomie et al.	Beck et al.	Gratzke et al.	Xie	Mendez et al.	Nguyen et al.
Reference No.	[5]	[43]	[10, 20]	[11]	[48]	[18, 19]	[12]	[25]	[15, 16]	[13]	[14]	[17]	[47]	[40]	[54]	[29–32]	[8, 9]
Welding Process — GTAW				•		•	•	•								•	
GMAW	•		•												•		•
SAW		•															
LBW									•	•	•	•	•	•	•		
EBW					•												
Material — Steels	•	•	•		•	•	•	•	•	•	•	•	•	•	•		•
Stainless steels					•			•	•	•	•	•	•		•		
Aluminium alloys											•		•	•	•	•	
Copper alloys														•	•		
Weld type — Bead on plate	•		•	•	•	•	•	•	•	•	•	•			•	•	•
Partial/full Pen. welds		•							•						•		
Keyhole/conduction					•								•		•		
Welding process parameters — Welding speed	•	•	•	•	•	•	•	•	•	•	•	•	•	•	•	•	•
Power/current/voltage	•	•	•	•	•	•	•	•	•	•	•	•	•	•	•	•	•
Plate surface condition	•																
Ar shielding gas	•		•	•		•	•	•									•
He shielding gas	•					•	•										•
Ar–O$_2$ shielding gas	•																
CO$_2$ shielding gas			•														
Flux		•	•														
Ambient pressure																	
Torch orientation	•							•									
Work piece orientation								•			•						•
Electrode tip geometry			•	•		•											
Electrode diameter			•	•		•	•			•	•						
Electrode gap						•	•										
Tandem heat sources					•							•					
Power ratio					•							•					
Dual heat sources gap									•			•					
Proposed models — Rayleigh instability	•													•	•		
Pressure balance		•															
Supercritical flow				•												•	
High velocity flow			•		•			•					•				
Curved wall jet																	•

6 Schematic diagram showing cylindrical inviscid fluid jet freely suspended in space with unperturbed radius *R* and length *l*, described in the Rayleigh jet instability model

these experimental results do not directly reveal the physical mechanisms responsible for the formation of these defects, e.g. they do not explain what causes the transition from good welds to undercutting or humping with increased welding speed.

Proposed mechanisms for formation of high speed weld defects

Understanding the mechanisms and driving forces responsible for undercutting and humping is essential if techniques for suppression or elimination of these defects are to be developed. While several attempts have been made to view the formation of undercuts and humping using high speed film[5,15,16] and video imaging,[8,9] these images are of the surface of a rapidly moving opaque fluid directly under an intense plasma arc light source. It is difficult to glean from such images the physical phenomena that are taking place during the formation of humping and undercutting. Nevertheless, various mechanisms for the formation of defects have been proposed based on such observations obtained from imaging of the weld pool, other experimental techniques and results and the final weld bead profiles.

Rayleigh jet instability model

Bradstreet[5] was the first to attempt to explain the humping and undercutting phenomena. Based on observations of the final weld bead profile, he suggested that the humping phenomenon was analogous to the Rayleigh jet instability model of a cylindrical inviscid fluid jet freely suspended in space.[35,36] The Rayleigh instability model is based on the conservation of mechanical energy and as shown in Fig. 6, it predicts that the lateral surface of the cylindrical jet will be unstable once its length *l*, exceeds its circumference $2\pi R$, where *R* is the radius of the cylindrical jet. The instability grows most rapidly when *l* is equal to $2 \cdot 9\pi R$[35,36] causing a periodic swelling and necking of the jet and eventual break-up of the jet into a stream of individual droplets. It should be noted, however, that in this highly idealised model, many important effects such as the imbalance of the forces between the top free surface and the bottom surface in contact with the solid fusion boundary, viscosity and viscous drag forces acting on the liquid at the fusion boundary as well as the effects of solidification on the time varying domain of the liquid jet are all ignored.

In the context of a weld, the similarity between the Rayleigh jet instability model and humping is based on observations of the periodic bead geometry of the molten weld metal behind the welding arc in the tail of the weld pool. At high welding speeds and currents, the top surface of the weld pool is believed to transform from a flat to a convex shape behind the arc where

surface tension forces draw the molten metal into a cylindrical shaped jet. The pressure inside this jet is increased owing to the need to balance surface tension forces.[37] Once the lateral surface instability begins, the molten metal flowing through the jet from the centre of the weld pool towards the tail of the weld pool will begin to form the periodic necking and swelling that is characteristic of the humped bead geometry. Bradstreet[5] argued that the combination of the small radius of the neck and the relatively cold underlying work piece results in premature solidification of the molten metal in the neck, thereby cutting off the fluid flow to the swelling. As welding continues, a new swelling or hump will form again once the jet reaches the critical length *l*.[5] This proposed Rayleigh instability model of humping was also adopted by Tsukamoto *et al.*[15] to explain humping in EBW of steel plate and by Simon *et al.*[38] in CO_2 LBW of metals.

There is ongoing debate about the validity of using the Rayleigh instability model to explain the driving forces responsible for humping. As originally proposed, the surface tension induced pressure in the swelling or hump is smaller than that in the neck because of the difference between their respective radii of curvature. Bradstreet[5] argued that this pressure difference was the driving force for the build-up of molten metal at the tail of the weld pool that ultimately forms the hump. On the other hand, Ishizaki[37] has theorised that the high internal pressure of the small molten droplets being transferred across the arc to the weld pool is the driving force responsible for the humping in GMAW. He argued that the high internal pressure in these droplets causes the molten metal to flow backward from the arc gouged region through the jet of molten metal and eventually to pile up forming a hump at the tail of the weld pool. According to Ishizaki,[37] the backward flow of molten metal will stop and another hump will form when the pressure inside the jet equals the pressure within these molten droplets. However, the relationship between surface tension generated pressure within the droplets and pressures within the weld pool is unclear because, unlike mass, momentum or energy, pressure in a fluid is not a conserved quantity.

Hügel *et al.*[39] have argued that humping in laser welds is caused by the surface tension at the keyhole rim and the shear force due to vapour flow inside the keyhole of the laser weld. These provide the driving force for the pile up of molten metal at the tail of the weld pool. Using a numerical model, they predicted a region of high metallostatic pressure at the tail of the weld pool. These results contradict previous suggestions by Bradstreet[5] and Ishizaki,[37] because the high local pressure at the tail of the weld pool should prevent further accumulation of molten metal.

Although the Rayleigh jet instability model may explain the periodic occurrence of the swellings in a humped weld, it cannot be used directly to predict the combination of welding process parameters that will result in a humped weld. Furthermore, the Rayleigh jet instability model assumes that the molten weld metal must have a cylindrical shape and be freely suspended in space.[35,36] With severe undercut, the molten weld metal does assume a shape that closely approximates an unsupported cylinder. For these welds, Bradstreet[5] obtained good correlation between the observed average
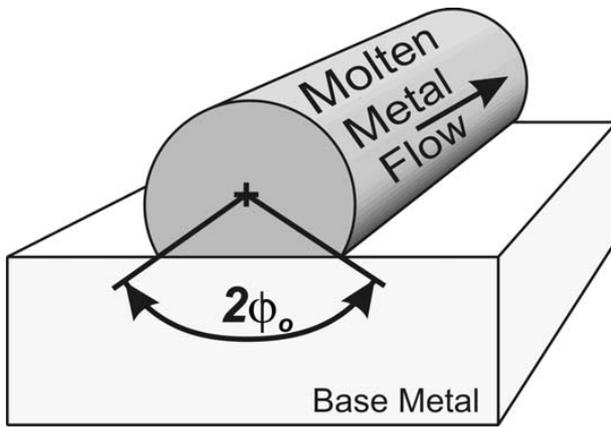
7 Subtended wetted angle $2\varphi_o$, as defined by Gratzke et al.[40]

hump spacing and the critical instability length predicted by the Rayleigh instability model. On the other hand, without severe undercut, the measured and calculated results were significantly different, although of approximately the same order of magnitude.[5]

To overcome the deficiency of the Rayleigh instability based model for humping noted by Bradstreet,[5] Gratzke et al.[40] introduced a correcting function $B(\varphi_o)$ and established a new instability criterion, i.e. humping will occur when

$$l > 2\pi \times R \times B(\varphi_o) \qquad (2)$$

where l and R are as depicted in Fig. 6 and $B(\varphi_o)$ is a correcting function which is dependent on the angle φ_o, as shown in Fig. 7. When the angle $\varphi_o=0$, the cylindrical jet only touches tangentially to a flat surface. This corresponds most closely to the free standing jet in the Rayleigh instability model. The main purpose of the correcting function $B(\varphi_o)$, is to account for the wetted perimeter that exists between the solid at the fusion boundary and the molten metal jet. Gratzke et al.[40] suggested that humping would occur when $B(\varphi_o)=1{\cdot}5$ (i.e. $\varphi_o \approx 60°$) for GMAW and when $B(\varphi_o)=2$ (i.e. $\varphi_o \approx 80°$) for LBW. However, these values were not validated experimentally.

By rearranging equation (2), Gratzke et al.[40] were able to define a critical ratio between the width and the length of the weld pool below which humping was predicted to occur. This model appears to be supported by Bagger et al.[41] observed reduction in the area and the width of the weld pool upon formation of a hump. These arguments suggest that maximising the width to length ratio of the weld pool during welding will suppress the formation of undercuts and humping. If this is true, then a side by side arrangement of two heat sources would be expected to increase the width to length ratio of the weld pool thereby allowing higher welding speeds. As discussed in the latter portion of the present review, the inline arrangement of the heat sources of a welding process with two heat sources (i.e. one heat source is in front of the other) has been shown to be effective in achieving higher welding speeds.[15,18,19] More experimental work is needed to examine the validity of this modified Rayleigh jet instability model and its ability to predict the observed effects of different welding process parameters on the humping phenomenon.

While studying the sweep deposition of molten wax on a flat surface, Gao and Sonin[42] observed that the resultant wax bead had periodic ripples at higher depositing frequencies of the molten wax droplets. The observed undulation of the wax beads was very similar to the humping phenomenon in a weld. Gao and Sonin[42] suggested that the formation of these undulations is similar to the Rayleigh jet instability. Schiaffino and Sonin[23] later demonstrated that the undulation of these wax beads would only occur if the initial contact angle between the liquid wax and the flat surface is $>\pi/2$ (90°). Using inviscid flow theory, Schiaffino and Sonin[23] showed some correlations between the wavelength of the undulations and the wavelength associated with the maximum growth rate of the instability.

The proposed instability theory by Schiaffino and Sonin[23] may not entirely explain the humping phenomenon in welding. As previously mentioned, by using reactive shielding gases, a low initial contact angle between the molten weld metal and the work piece can be achieved. Despite the low initial contact angle, humping will eventually occur at higher welding speeds. In fact, as observed by Bradstreet,[5] the molten metal of a humped weld produced with reactive shielding gas had a small contact angle with the unmelted based metal. This is indicative of good wetting between the molten weld metal and the unmelted base material. This would suggest that the instability of the weld bead and humping is not based solely on the contact angle between the liquid metal and the work piece.

Albright and Chiang[14] used the Rayleigh jet instability model to predict the onset of blowhole defects in high speed LBW of thin 304 stainless steel sheets. They used this model to predict the break-up length of a cylindrical fluid jet into individual droplets l_c, as shown in Fig. 6. The driving force for this is minimisation of the overall surface energy. The break-up length can be calculated as follows

$$l_c = \frac{12v}{[\gamma/(8\rho R^3)]^{1/2}} \qquad (3)$$

where l_c (m) is the break-up length of the liquid jet; γ (N m^{-1}) is the surface tension of the fluid; ρ (kg m^{-3}) is the liquid density; R (m) is the nozzle or initial jet radius and v (m s^{-1}) is the liquid flow speed, which was taken as the welding speed.[14] If the weld pool was shorter than the break-up length l_c, then the weld pool was stable and blowholes would not form. On the other hand, the weld pool would be unstable when its length was longer than the break-up length. Within an unstable weld pool, the molten metal is predicted to swell into spherical balls separated by through thickness holes or blowholes. Albright and Chiang's results[14] showed that the break-up length l_c, predicted by the Rayleigh instability model could be used to predict the occurrence of blowholes in welds.

Arc pressure model

Although it is difficult to make direct observations of fluid flow in an arc weld pool, it is generally believed that the undercut and humping phenomena are initiated by events taking place in the weld pool directly underneath the welding arc. For example, Yamauchi and Taka[18,19] and Paton et al.[43] considered the static balance between the arc pressure and the metallostatic pressure of the
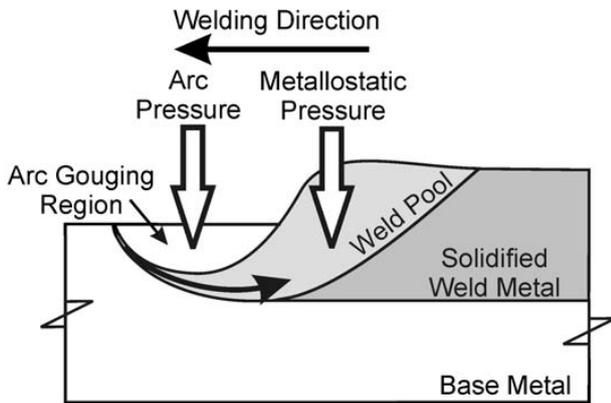
8 Schematic diagram illustrating balance between arc pressure and metallostatic pressure of molten weld metal during arc welding

9 Arc gouging region, trailing region, rim of molten weld metal and transition line in high speed GTA weld as defined by Yamamoto and Shimada[11] and Mendez et al.[29–32] for their supercritical flow models of humping

molten metal at the tail of the weld pool to be responsible for the final weld bead profile and humping. A schematic diagram of the static pressure balance is shown in Fig. 8. According to their pressure balance model of humping, when the metallostatic pressure of the molten metal exceeds the arc pressure, a thick layer of molten metal will exist beneath the arc. This will result in good weld bead geometry. Conversely, when the arc pressure is much greater than the metallostatic pressure, the pressure from the arc depresses the weld pool surface and creates a crater with a very thin layer of molten metal. Most of the remaining molten metal is displaced toward the tail of the weld pool. In this latter situation, the arc gouged crater is not filled at the lateral weld edges by the displaced molten metal prior to solidification and therefore undercutting occurs. Based on the pressure balance model, therefore, higher welding speeds can be achieved by selecting process parameters that reduce the overall arc pressure.

The impinging of the high velocity plasma jet on the weld pool surface generates the arc pressure that acts on the free surface to create a depression in the weld pool surface.[18,19,24,44] In the GMAW process, the momentum transfer from the stream of molten filler metal droplets also contributes to the depression of the weld pool surface. Higher welding speeds and currents have been shown to reduce the metallostatic pressure of the molten metal within the weld pool[43] and to increase the arc pressure.[12,18,19,24,45,46] The arc pressure is also strongly dependent on the physical properties of the shielding gas.[12,19,24] For example, higher welding speeds have been obtained by switching from Ar to the lower molecular weight He shielding gas when GTAW of stainless steel[11,24,45] or by welding in a low ambient pressure environment.[25]

The pressure balance model attributes the formation of undercut at high welding speeds to the inability of molten weld metal to laterally fill the crater gouged out by the welding arc before the completion of solidification. However, this is a steady state model that does not explain the swellings and the periodic behaviour of the humping phenomenon because it does not include the interactions between fluid flow, surface tension and solidification of the molten weld metal during humping. Finally, because the model is qualitative, it cannot be used to predict the actual welding conditions that will initiate the formation of undercuts and humping.
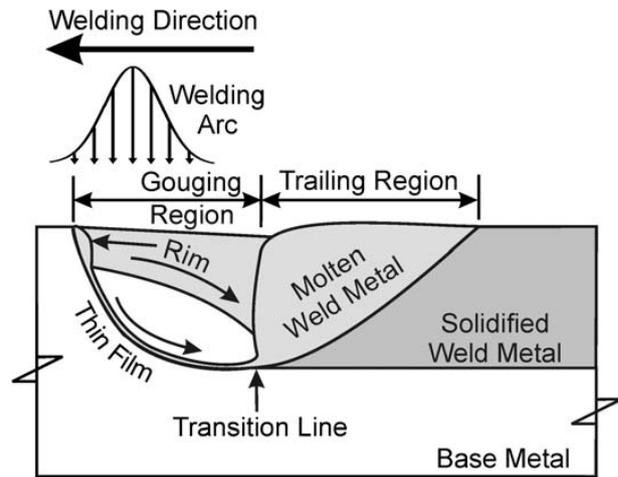
Supercritical flow model

In an attempt to include the influence of the molten weld metal flow in GTA weld pools on the undercutting and humping phenomena, Yamamoto and Shimada[11] have proposed a supercritical flow model for humping. Under the influence of high arc currents and pressures, they noted that GTA weld pool surfaces are significantly depressed and that only a very thin layer of molten metal exists within the arc gouged region of the weld pool as shown in Fig. 9. Because most of the melted base metal must flow from the front of the weld pool to the tail of the weld pool through this thin film or wall jet, the flow velocities through this wall jet are very high. Yamamoto and Shimada[11] argued that humping occurs when the molten metal velocity in the wall jet exceeds a critical value and a hydraulic jump forms in the weld pool with the swellings similar to those observed in humped welds. The supercritical flow model can also be applied to non-autogenous welding processes such as the GMAW process.

Although the supercritical flow model appears to be able to predict the fluid flow conditions that must exist within the weld pool for humping to occur, it does not explain the observed periodic nature of humps nor does it provide the link between the principal welding process parameters and the fluid flow conditions that will exist within the weld pool when humping occurs. Although the molten weld metal velocity field can be obtained from numerical simulations such as that of Beck et al.,[47] the results cannot be readily verified, because the molten weld metal velocities are difficult to measure. Therefore, the supercritical flow model cannot as yet be used directly to predict the conditions that will cause humping on the basis of the principal welding process parameters.

Mendez et al.[29–32] have attempted to explain the periodic nature of humping by modifying the supercritical flow model by Yamamoto and Shimada.[11] In this modified model, the weld pool is divided into two main regions; an arc gouged region at the front of the weld pool directly under the arc and a trailing region at the weld pool tail as shown in Fig. 9. At high welding
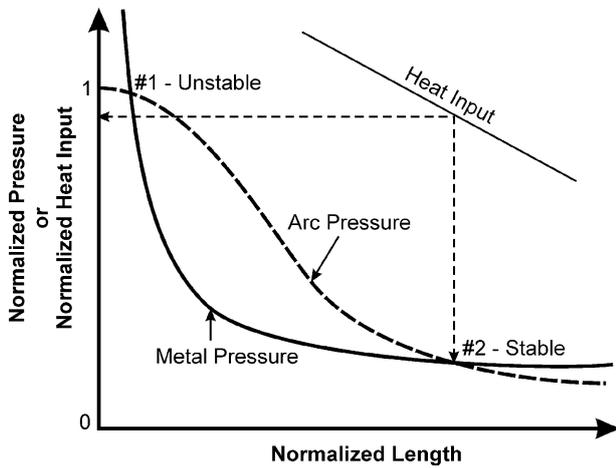
10 Relationship between arc pressure and metal pressure in GTA weld as presented by Mendez *et al.*[29–32]

currents, arc forces depress the weld pool surface and create a very thin film of molten metal underneath the arc. On the upper portion of the weld pool wall, however, a slightly thicker wall jet or layer of molten metal has been observed to exist around upper rim of the weld pool fusion boundary. It is thought that this layer of molten metal around the rim of the weld pool is thicker because of the contact angle and capillary forces acting on the liquid surface where it contacts the solid base metal and because it is further away from the arc where arc forces that depress the molten metal surface are weakest. During welding, molten metal flows from the front to the tail of the weld pool through a combination of the rim and the thin film wall jets. The trailing region at the tail of the weld pool contains the bulk of molten weld metal. As shown in Fig. 9, these two regions meet at a distinct transition line.

According to Mendez *et al.*,[29–32] the location of the transition line between the arc gouged and the trailing regions determines the onset of the humping weld defect. The location of the transition line can be estimated from the force created by the arc pressure and the combined force caused by the metallostatic pressure of the molten weld metal and the capillary effect. The arc force displaces the transition line toward the back of the weld pool and away from the welding arc, while the metallostatic pressure of molten weld metal and capillary force resist this rearward displacement.

Figure 10 shows generalised relationships between the normalised arc pressure, the normalised metal pressure and the normalised heat input plotted against the normalised length of the arc gouged region respectively. In this case, the arc pressure was assumed to be a Gaussian distribution and was normalised with respect to the predicted peak pressure directly under the electrode and the assumed Gaussian distribution heat input has been normalised with respect to the peak heat flux from the arc again, directly under the electrode. The normalised length scale l, is the size of the gouging region of the weld pool L, normalised with respect to the length scale of the pressure distribution L_P, i.e. $l=L/L_P$. These relationships were obtained by using a magnitude scaling technique.[29–32] In this plot, the metal pressure line represents the combined force of the metallostatic pressure of the molten weld metal and the capillary effect. As labelled in Fig. 10, there are two intersections

between the arc and the metal pressure curves. At intersection #1, the relationship between the arc pressure and the metal pressure is unstable. Any disturbance will either eliminate the arc gouged region owing to the increased metal pressure and the reduced arc pressure or develop a gouged region owing to higher arc pressures and reductions in metal pressure. For the first scenario, humping will not form. If the latter scenario occurs, the arc pressure and the metal pressure curves will cross at intersection #2. At this intersection, the relationship between the arc pressure and the metal pressure is stable. Any reduction in the length of the gouged region will increase the arc pressure that pushes the transition point backward. As a result, the arc gouged region will regain its original length. On the other hand, an elongation of the arc gouged region will increase the metal pressure that pushes the transition line forward and eliminates any length increase.

Under normal welding conditions, the arc gouged region does not extend very far from the arc. At higher welding speeds or currents, however, the higher arc pressure moves the arc gouged region further back towards the tail of the weld pool, therefore pushing the trailing region further back and away from the welding arc. As shown in Fig. 10, the amount of normalised heat input received at intersection #2 between the arc pressure and the metal pressure curves is less than unity. Therefore, the transition line between the arc gouged region and the trailing regions is normally located at the tail portion of the heat input distribution. With less local heat input from the arc, the thin film solidifies, thereby preventing the molten metal in the thin film from flowing to the back of the weld pool. As welding continues and molten metal continues to flow towards the tail of the weld through the thin film and rim, a new hump begins to form at the point where the thin film solidified and the cycle is repeated.

In the modified supercritical flow model by Mendez *et al.*[29–32] the effects of fluid motion, solidification of molten metal in the thin film and the balance between arc pressure and metallostatic pressure effects on the undercut and humping phenomena have been considered. However, in its present form, the model cannot predict the onset of humping based on the independent welding parameters used and does not directly suggest any solutions to elimination or suppression of undercut and humping. As well, there is heavy emphasis placed on the solidification of the thin film directly underneath the welding arc while the significant role of the rim in transporting liquid metal to the trailing region is ignored.

Curved wall jet model

Based on video imaging of GMA welds made on mild steel plates and corroborating experiments, Nguyen *et al.*[8,9] have recently proposed a curved wall jet model of humping in non-autogenous welding processes such as GMAW. Figure 11 shows schematic diagrams of longitudinal sections of welds produced using the same welding parameters, but at low and high welding speeds respectively. On these diagrams, d is the longitudinal distance along the weld centre line from the leading edge of the weld pool to the location where the filler metal droplet impinges the top surface of the weld pool. As illustrated in Fig. 11*a*, during low speed welding, the molten weld metal is contained within a large weld pool
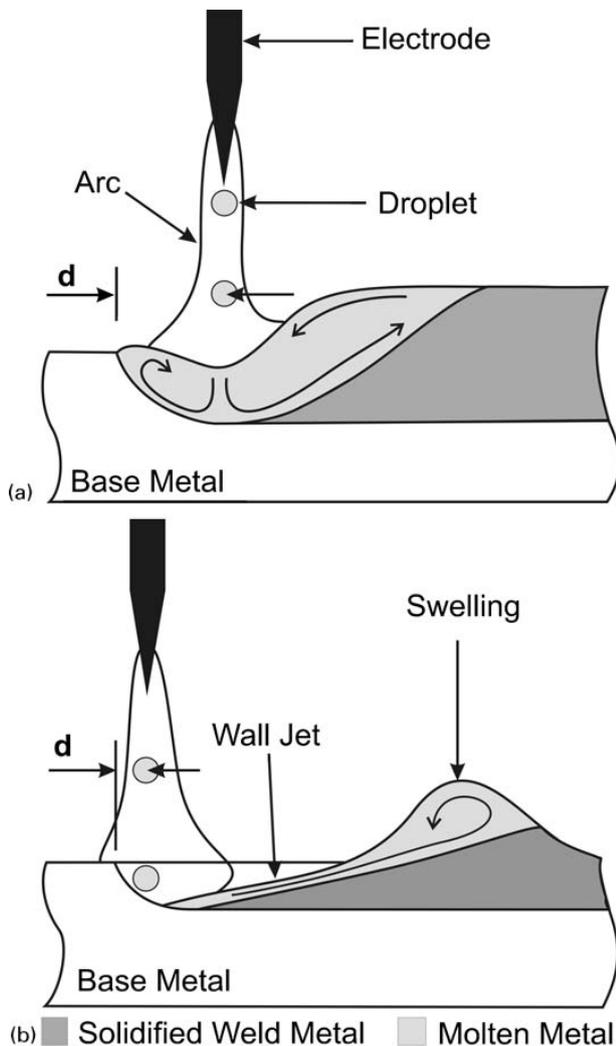
11 **Longitudinal sections of GMA weld pool and filler metal droplet impingement locations at *a* low welding speeds and *b* high welding speeds with wall jet and humping (after Nguyen *et al.*[8,9])**

underneath the welding arc. The depression of the free surface of the weld pool due to the arc force and the filler droplet momentum is possible, but limited by the forward recirculation of the molten weld metal. This relatively large pool of molten metal absorbs and dissipates the momentum of the incoming filler metal droplets in the GMAW process and resists the effects of the arc forces. Consequently, the backward momentum of molten metal within this weld pool is low and there is little chance of forming a humped weld.

As illustrated in Fig. 11*b*, at high welding speeds, the weld pool becomes elongated, shallow and narrow. Also, the electrode, the welding arc and the metal droplet stream move forward and closer to the leading edge of the weld pool, i.e. *d* decreases. Nguyen *et al.*[8,9] observed an inverse relationship between d and the welding speed. Owing to the reduction in penetration and volume or mass of molten metal in the weld pool, the combined actions of the arc force and the droplet momentum create a depression or gouged region at the front of the weld pool that contains a thin layer of liquid metal underneath the welding arc. Without the presence of a thick liquid layer underneath the welding arc, the momentum of the incoming filler metal droplets are not

absorbed or dissipated. Rather, the droplets hit the sloping leading edge of the weld pool (see Fig. 11*b*) and this molten filler metal is then redirected towards the tail of the weld pool at high velocity through a semicircular curved wall jet frequently similar in shape to that shown in Fig. 7, dragging with it any liquid metal in the front of the weld pool from the melting base metal. This high velocity, rearward directed flow of molten weld metal in the weld pool is consistent with numerical simulations by Beck *et al.*[47] and observations in tandem EBW by Arata and Nabegata.[48] Backfilling of the front portion of the weld pool as described by Bradstreet[5] does not occur because the recirculated molten weld metal fails to keep up with the forward moving welding arc and is pushed or held back by the high velocity and momentum of the backward directed fluid flow within the wall jet. At the tail of the weld pool, the molten weld metal accumulates to form a swelling that is drawn into a spherical bead shape by surface tension as molten metal is fed into the swelling from the front of the weld pool through the wall jet. Therefore, the momentum of the backward flow of molten weld metal is responsible for not only the initial formation, but also the growth of the swelling.

Although the swelling increases in size as molten metal flows into it, the new swelling is stationary with respect to the base plate. As the welding arc continues to move to the left along the weld joint, the wall jet becomes increasingly elongated and the thermal mass of molten metal inside the wall jet becomes distributed over a longer distance until continued solidification of the weld and the molten metal in the elongated wall jet chokes off the flow of molten metal to the swelling. Solidification of the wall jet forms the valley typically observed between swellings in a humped GMA weld bead such as that shown in Fig. 2. Initiation and growth of a new swelling closer to the arc and further along the weld bead occurs very soon after fluid flow in the wall jet is choked off. This sequential formation of a swelling or hump at the tail of the weld pool and solidification of the wall jet is a periodic phenomenon that results in the formation of humping in GMA welds. Nguyen[8] has shown that the humping frequency of this periodic phenomenon increases with increasing welding speed or decreasing welding power.

The studies and proposed phenomenological models for undercut and humping in various welding processes are summarised in Table 1. The arc pressure model,[43] the supercritical flow model[11] and the modified supercritical flow model[29–32] were developed from observations of the autogenous GTAW process in which the welding arc plays a critical role in the formation of high speed weld defects. However, these models may not be as directly applicable to the autogenous, high energy density processes such as LBW and EBW, especially when keyhole mode welding is used. In both of the latter welding processes, the material laser beam interaction is fundamentally different from that found in arc welding processes. The Rayleigh jet instability model by Bradstreet,[5] the pressure balance model by Paton *et al.*[43] and more recently the curved wall jet model by Nguyen *et al.*[8,9] have been used in attempts to explain the undercutting and humping phenomena in non-autogenous welding processes such as GMAW and SAW. In these processes, the momentum from the filler metal droplets also plays a role in the heat and mass

transfer responsible for these defects. It is possible that these proposed models are quite process specific and that different physical phenomena are responsible for humping and undercutting in the various autogenous and non-autogenous fusion welding processes.

The proposed phenomenological models of undercutting and humping suggest that fluid flow and the high velocity and momentum of the backward directed flow of molten metal in the weld pool, arc pressure, metallostatic pressure, capillary forces and lateral instability of a cylindrical or curved wall jet of molten weld metal and the periodic solidification of this wall jet are responsible for the formation of humping and undercutting. However, the exact mechanism is unclear and is still being debated. Although some of the proposed models can provide plausible explanations of the periodic behaviour of the humping phenomenon, their ability to predict the onset of humping or undercutting using the independent welding parameters have not been experimentally validated. More importantly, from a technological perspective, these models do not always directly suggest possible techniques that might be used to achieve higher welding speeds without the formation of undercut or humping weld defects.

Techniques and processes for higher welding speeds

The lack of a comprehensive phenomenological model for the formation of humps and undercuts at higher travel speeds does not prevent the unrelenting search for welding techniques or processes to achieve higher productivity. Over the years, practitioners have discovered several welding techniques and processes that can be used to increase the overall productivity without sacrificing weld quality. Although it is frequently difficult at the present time to properly explain why these techniques work, a discussion of these welding techniques and processes is valuable. These modified welding techniques and processes may offer useful insights into the formation and the suppression of high speed weld defects such as undercut and humping.

Experimental results from past investigators have demonstrated the significant effect of shielding gas on the suppression of high speed welding defects.[5,8–12] Savage *et al.*[12] reported that higher GTAW speeds were achieved when He shielding gas was used instead of Ar during bead on plate welding of stainless steel. Although the measured arc force was not altered,[12] the arc pressure was uniformly distributed over a larger area due to the lower density and higher viscosity of He compared with Ar.[45] As a result, the overall arc pressure was reduced allowing higher welding speeds to be used without the formation of defects. Yamauchi and Taka[19] have also shown that measured arc pressures in GTAW arcs are significantly lower when He is used instead of Ar with conical shaped electrodes; however, there was little difference in arc pressures of the Ar or He arcs when hollow electrodes were used.

In GMAW with CO_2 shielding gas, the buried arc technique has been reported as an effective means of achieving higher welding speeds and filler metal deposition rates.[5,10] With this technique, the arc is actually located beneath the original surface of the work piece during welding. This reduces the weld spatter and
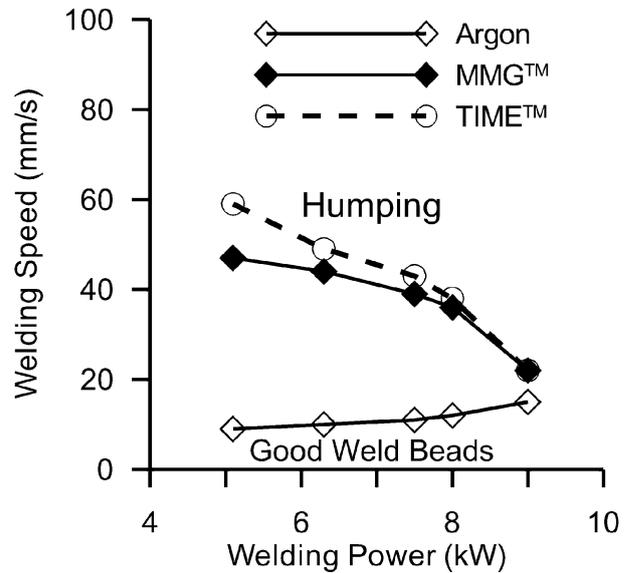
12 Limiting welding speeds above which humping was observed versus welding power when making GMA welds in plain carbon steel using Ar and reactive shielding gases MMG^{TM} and TIME^{TM} (taken from Nguyen *et al.*[8,9])

increases the metal deposition rate. In addition, the overall arc pressure may be reduced since the cathode is located within the weld pool crater.[20] This is consistent with the arc pressure and supercritical models wherein a reduction in arc pressure is predicted to decrease the arc gouging directly under the arc, thereby suppressing the formation of humps and undercuts to higher welding speeds and allowing improvements in productivity.[43]

During GMAW of mild steel, Bradstreet[5] observed the beneficial effects of using a small amount of O_2 in the Ar shielding gas. He attributed this to improved wetting at the solid/liquid interface within the weld pool when Ar with $2–5\%O_2$ shielding gas was used. These results are consistent with the current practice of using a small percentage of O_2 in pure Ar shielding gas to improve the wetting of molten metal in the GMA weld pool.[49] These results are also consistent with the Rayleigh jet instability model, where the improved wetting at the solid/liquid interface would increase the equivalent radius and therefore the overall circumference of the cylindrical jet. Moreover, according to Schiaffino and Sonin,[23] a low contact angle between the molten weld metal and the unmelted work piece will suppress the hump formation. As a consequence, higher welding speeds can be achieved without defect formation when reactive shielding gas is used.

Figure 12 shows the limiting welding speeds above which humping was observed by Nguyen *et al.*[8,9] versus welding power for GMA welds produced in mild steel plate when using Argon and two reactive shielding gases, MMG^{TM} (Ar–8CO$_2$) and TIME^{TM} (Ar–8CO$_2$– 26·5He–0·5O$_2$) shielding gases. When using MMG^{TM} and TIME^{TM} shielding gases, the limiting welding speed decreased as the welding power increased. This trend is very similar to those reported in previous studies of the humping phenomenon.[12–17,20] However, at the lowest powers, use of reactive MMG^{TM} and TIME^{TM} shielding gases suppressed humping and allowed up to 400% higher welding speeds than are possible with pure Argon
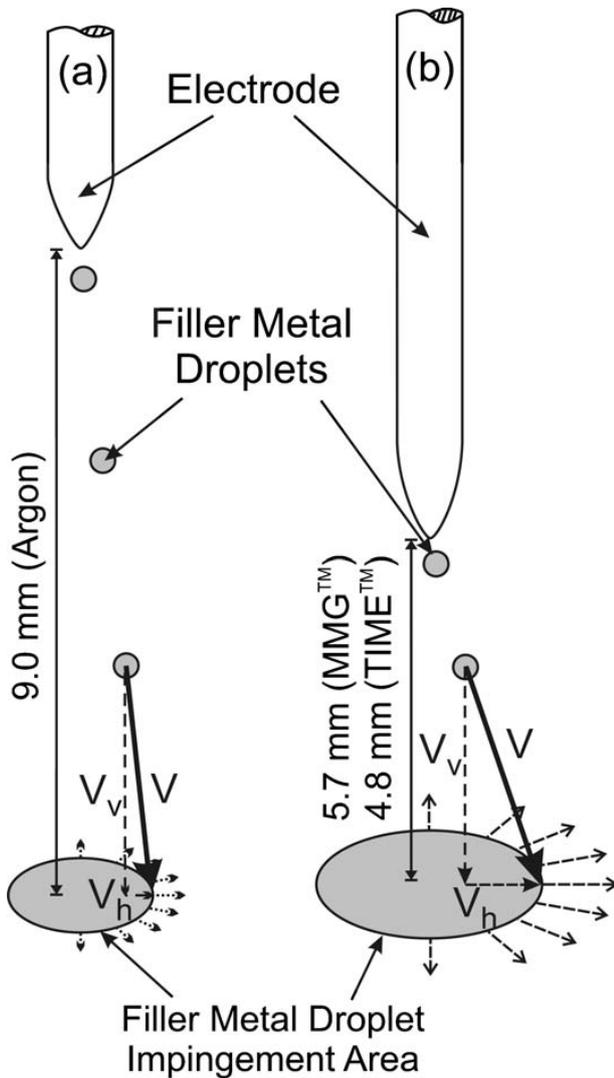
13 Differences in arc gaps and overall velocity *V* and velocity components *V*ᵥ and *V*ₕ of filler metal droplets during GMAW when using Ar (a) and reactive (b) MMG™ and TIME™ shielding gases (taken from Nguyen *et al.*[8,9])

shielding gas. This significant improvement in productivity when using the reactive shielding gases was explain based on video observations of the metal droplet distribution patterns when using the different shielding gases. As shown in Fig. 13, with reactive shielding gases, the arc gap is shorter and the stream of molten filler metal droplets from the electrode was less focused and was spread out over a larger area of the weld pool. This caused an increase in weld width relative to welds made with Ar shielding gas. They suggested that the smaller arc gap and therefore lower arc forces, the larger filler metal droplet impingement area, the less focused and more lateral flow of molten filler metal droplets and the extra opposing viscous drag force from the large fusion boundary all reduced the depression of the weld pool surface and the overall momentum of the backward flow of molten weld metal in the weld pool thereby allowing significantly higher welding speeds without humping.[8,9]

The tandem arrangement of GTAW torches,[18,19] GMAW torches,[50,51,52] laser beams[53,54] and electron beams[15,48] have also been shown to be very effective in delaying the onset of humping and undercuts to higher welding speeds. In recent developments, two GMAW electrodes, arranged in line with the welding direction, were reported to provide between two and three times higher welding speeds and filler metal deposition rates without the occurrence of defects such as undercut and humping.[50,52] This new GMAW variation is often referred to as tandem wire GMAW. In tandem wire GMAW, the leading power supply and wire feed rate are adjusted to achieve the desired weld penetration and filler metal deposition rate. A short arc length, long electrode stickout and high welding current are commonly used.[51] The trailing power supply and electrode feed rate are adjusted to achieve the desired weld bead profile and to prolong the degasification time.[51,52] The process parameters of the trailing electrode are set to produce less severe welding conditions. In fact, there appears to be an optimal ratio between the power levels of the two GTAW electrodes,[18] the two GMAW electrodes[50–52] or between the two beams in the dual beam EBW[48] and dual beam LBW[27,28] welding processes.

Although the addition of the second heat source into a common weld pool allows significantly higher welding speeds to be used before undercutting or humping occurs, the exact mechanism responsible for suppressing these weld defects and the actual roles of the second electrode or beam are not thoroughly understood. Yamauchi and Taka[18,19] and Ueyama *et al.*[52] suggested that the trailing arc stopped or significantly reduced the backward flow of molten metal caused by the arc forces from the leading arc. This is consistent with Nguyen *et al.*[8,9] curved wall jet model of humping. Dilthey *et al.*[53] suggested that the main functions of the second beam in the tandem dual beam LBW process are to reheat the weld metal at the tail of the weld pool and to allow time for surface tension and gravitational forces to smooth out the top surface of the weld pool prior to solidification, thereby avoiding the formation of geometric defects such as undercuts or humps. On the other hand, Hügel *et al.*[39] suggested that the second beam in tandem dual beam LBW enlarges and stabilises the keyhole. The larger keyhole is then responsible for an increase in the weld pool cross-section and a reduction in the fluid velocity and pressure at the tail of the molten weld pool. Both of these changes help to suppress the formation of defects at high welding speeds. Using real time high speed X-ray imaging, Iwase *et al.*[55] have shown that the distance between the two beams influences the top weld width and the stability of the keyhole during partial penetration, bead on plate, dual beam laser welding of 5xxx series aluminium alloy plate. Deutsch *et al.*[27] and Punkari *et al.*[28] have also observed the beneficial effects of the second tandem beam on keyhole stability and weld bead quality during dual beam Nd:YAG laser welding of AA5182 and AA5754 aluminium alloy sheet. They found that good quality weld beads were produced in these alloys provided that the lead/lag beam power ratio was ≥1. This is similar to the lead/lag power ratio frequently used in tandem GMAW.[51,52]

Using a tandem dual beam CO_2 LBW process, Xie[54] has shown that undercut and humping defects in plain carbon steel and aluminium LBW welds can be significantly reduced or eliminated. He argued that the effects of the second beam on the welding process depended on the relative distance between the two laser beams.

Similar to Dilthey *et al.*,[53] he suggested that when the beams were far apart, the second beam reheats and smoothes the weld bead surface, effectively eliminating any undercut or humping defects that had been created by the leading beam. Alternatively, when the beams are close together, the second beam acts to stabilise the keyhole and enlarge the weld pool thereby suppressing the formation of the undercut and humping defects until higher welding speeds are used. This is similar to the arguments of Hügel *et al.*[39] When the distance between the beams is intermediate to these two cases, Xie[54] argued that the second beam creates a second keyhole in the weld pool behind the keyhole created by the leading beam. This is similar to the results of Arata *et al.*[48] which showed that the speed at which humping occurred in EBW welding could be increased up to 50% by using a tandem dual beam EBW system. They attributed the suppression of undercutting and humping to the change in momentum of the backward flow of the molten weld metal as it was forced to flow around the second beam cavity. The second keyhole diverts the flow of superheated liquid metal towards the lateral solid/liquid interfaces and remelts any previously solidified metal. As a result, the flow channel is broadened, thereby reducing the pressure and velocity of the fluid stream. With reductions of both the pressure and velocity, the molten weld metal will not accumulate to form a hump at the tail of the weld pool. The laterally diverted flow also prevents the formation of undercut.

The techniques described above and the related explanations for why they are able to effectively suppress the formation of the undercut and humping weld defects suggest that the backward momentum of the molten weld metal is a very influential factor. The ability to slow down the molten metal as it is being displaced at high velocities toward the tail of the weld pool appears to be the key to suppressing or even eliminating these high speed welding defects. This is supported by the work of Beck *et al.*[47] and was utilised by Kern *et al.*[56] in CO_2 LBW of construction steel. In the numerical simulations by Beck *et al.*,[47] a high velocity jet of molten metal directed toward the tail of the weld pool was predicted. This flow caused a steady accumulation of the molten metal and subsequent formation of a hump. According to Beck *et al.*,[47] any technique that will reduce the flow velocities of the rearward directed jet would lead to the suppression of humping. For example, by applying a magnetic field transverse to the welding direction, Kern *et al.*[56] were able to suppress the formation of humping in CO_2 laser welding of fine grained construction steel under some conditions. They hypothesised that the transversely imposed magnetic field altered the fluid flow profile within the weld pool and that this was responsible for the elimination of humping in their laser welds. At the same time, the high width to length ratio, also recommended by Gratzke *et al.*,[40] widens the weld pool and therefore slows the velocity of the backward flow of molten weld metal. Ueyama *et al.*[52] showed that there was always an optimum combination of GMAW trailing torch push angle, distance between the two GMAW electrodes and ratio of leading/trailing arc currents that would facilitate the highest welding speed without humping. Finally, Nguyen *et al.*[8,9] showed that the welding position and orientation of the work piece relative to gravity affects the backward flow of molten weld metal and the critical welding speed at which humping occurs during GMAW of mild steel. With 10° downhill welding position, the gravitational force weakened the backward flow of molten weld metal and allowed significantly higher welding speeds without the formation of humping. Conversely, 10° uphill welding position strengthened the backward flow of molten metal within the weld pool and caused humping to occur at much lower welding speeds. Therefore, higher welding speeds and improved productivity is possible by orienting the weldment such that welding is done in the downhill position. Based on these arguments and observations, future experimental work and models should be designed to carefully examine the role of molten metal fluid flow behaviour and its influences on the formation of undercut and humping weld defects.

The weld joint geometry has also been used to advantage to confine and restrict the molten weld metal flow in the weld pool, thereby suppressing the formation of undercut and humping defects.[16,57] Tsukamoto *et al.*[16] argued that a deep and narrow square groove prevents the molten metal from behaving as a cylindrical jet, which, according to the Rayleigh jet instability model, is a prerequisite for the formation of defects. However, it is not unreasonable to argue that the additional wetted contact with the fusion boundary provided by the groove increases viscous drag thereby decreasing the velocity of the molten metal and providing stability to the cylindrical jet.[35] Furthermore, according to Shannon,[57] certain weld joint geometries can result in wider weld pools. This will reduce the velocity of the molten weld metal towards the tail of the weld and therefore suppress the humping phenomenon.

In tandem electrode GTAW, tandem wire GMAW and dual beam EBW, the trailing electrode or beam is normally pointed in the direction of travel. This improves the final weld bead appearance.[18,19,48,50,52] Similarly, in multi-electrode SAW, forward deflection of the trailing arc has been shown to flatten the weld bead and eliminate weld defects such as undercut and humping at high welding speeds.[58] The forward deflection of the welding arc was also reported to be beneficial in obtaining higher welding speeds in single wire GMAW[5] whereas a lagging torch angle was found to promote undercutting and humping at much slower welding speeds. These observations suggest that the forward pointing of the trailing electrode or the trailing beam in tandem processes will influence the overall arc pressure or the backward momentum of the fluid flow within the weld pool and have a beneficial impact on the formation of hump and undercut at high welding speeds. This concept merits further investigation.

Several welding techniques and processes have been identified as being capable of suppressing the formation of undercutting and humping thereby permitting higher welding speeds and increased productivity. Although previously proposed phenomenological models of these defects are unable to comprehensively explain the apparent success of these techniques and processes, the benefits appear to be derived from their ability to slow down the backward flow of molten weld metal. These welding techniques and processes have revealed useful insights into the formation of high speed weld defects.

Further work is needed to examine the influence of the backward flow of molten weld metal on the formation of weld defects and to derive models that can predict the occurrence of undercutting and humping on the basis of the independent welding process parameters.

Concluding remarks

The formation of high speed weld defects such as undercutting and humping is a very complex phenomenon and dependent on many process parameters. However, in previous investigations, the influences of various welding parameters and their interactions on the formation of the weld defects were not always fully documented. As a consequence, it is difficult from the experimental results presented in these individual studies to derive techniques, other than reducing the welding speed, that can be used to eliminate or to suppress these weld defects.

Over the years, various conceptual models have been proposed to explain the humping phenomenon. These models suggest that fluid flow and the high velocity and momentum of the backward directed flow of molten metal in the weld pool, arc pressure, metallostatic pressure, capillary forces and lateral instability of a cylindrical or curved wall jet of molten weld metal and the periodic solidification of this curved wall jet are responsible for the formation of humping and undercutting. Some models suggest that at high welding speeds and welding currents, a very thin film of molten weld metal exists underneath the arc and that the molten weld metal is displaced at very high velocities toward the tail of the weld pool through this thin film or curved wall jet. The backward momentum of the molten metal appears to be a critical factor, because several welding techniques and processes have been demonstrated to be effective in suppressing weld defects by slowing down the backward flow of molten weld metal. Nevertheless, the exact formation mechanism of high speed weld defects for each different welding process is unclear and is still being debated. Although some of the proposed models can provide plausible explanations to the periodic behaviour of the humping phenomenon, their ability to predict the onset of humping or undercutting has not been proven experimentally. From a technological perspective, most of these models do not directly provide nor comprehensively explain possible techniques or processes that might be used to achieve higher welding speeds without the formation of defects such as undercut and humping.

Acknowledgements

References

1. D. T. Swift-Hook and A. E. F. Gick: *Weld. J.*, 1973, **52**, (11), 492–499.
2. P. W. Fuerschbach: Proc. Symp. TMS Fall Meet., (ed. M. J. Cieslak *et al.*), 21–29; 1992, Cincinnati, OH, The Minerals, Metals and Materials Society.
3. D. Rosenthal: *Weld. J.*, 1941, **20**, 220–234.
4. C. M. Adams, Jr: *Weld. J.*, 1958, **37**, (5), 210–215.
5. B. J. Bradstreet: *Weld. J.*, 1968, **47**, (6), 314–322.
6. 'Welding handbook', Vol. 1, 'Welding science and technology', (eds C. L. Jenny and A. O'Brien) 9th edn, 805; 2001, Miami, FL, American Welding Society.
7. H. R. Shakeri, Y. Lee, M. J. Worswick, F. Feng, W. Christy and J. A. Clarke: *SAE Trans. J. Mater. Manuf.*, 2001, **110**, 101–110.
8. T. C. Nguyen: 'Weld defects in high-speed gas metal arc welding', PhD thesis, University of Waterloo, ON, Canada, 2005.
9. T. C. Nguyen, D. C. Weckman, D. A. Johnson and H. W. Kerr: *Sci. Technol. Weld. Join.*, 2005, **10**, (4), 447–459.
10. K. Nishiguchi, K. Matsuyama, K. Terai and K. Ikeda: Proc. 2nd Int. Symp. on 'Advanced welding technology', Osaka, Japan, August 1975, Japan Welding Society, Paper 2-2-(10).
11. T. Yamamoto and W. Shimada: Proc. 2nd Int. Symp. on 'Advanced welding technology', Osaka, Japan, August 1975, Japan Welding Society, Paper 2-2-(7).
12. W. F. Savage, E. F. Nipples and K. Agusa: *Weld. J.*, 1979, **58**, (7), 212–224.
13. S. Hiramoto, M. Ohmine, T. Okuda and A. Shinmi: Proc. Int. Conf. on 'Laser advanced material processing: science and application', Osaka, Japan, May 1987, High Temperature Society of Japan and Japan Laser Processing Society, 157–162.
14. C. E. Albright and S. Chiang: *J. Laser Appl.*, 1988, **1**, (1), 18–24.
15. S. Tsukamoto, H. Irie, M. Inagaki and T. Hashimoto: *Trans. Natl Res. Inst. Met.*, 1983, **25**, (2), 62–67.
16. S. Tsukamoto, H. Irie, M. Inagaki and T. Hashimoto: *Trans. Natl Res. Inst. Met.*, 1984, **26**, (2), 133–140.
17. M. Tomie, N. Abe and Y. Arata: *Trans. JWRI*, 1989, **18**, (2), 175–180.
18. N. Yamauchi and T. Taka: IIW document 212G-437-78, 1978.
19. N. Yamauchi and T. Taka: IIW document 212G-452-79, 1979.
20. K. Nishiguchi and A. Matsunawa: Proc. 2nd Int. Symp. on 'Advanced welding technology', Osaka, Japan, August 1975, Japan Welding Society, Paper 2-2-(5).
21. V. R. Dillenbeck and L. Castagno: *Weld. J.*, 1987, **66**, (9), 45–49.
22. S. Subramaniam and D. R. White: *Metall. Mater. Trans. B*, 2001, **32B**, (2), 313–318.
23. S. Schiaffino and A. A. Sonin: *J. Fluid Mech.*, 1997, **343**, 95–110.
24. J. F. Lancaster (ed.): 'The physics of welding', 2nd edn, 1986, Oxford, Pergamon Press.
25. W. Shimada and S. Hoshinouchi: *J. Jpn Weld. Soc.*, 1982, **51**, (3), 280–286.
26. N. Abe, M. Tomie and Y. Arata: *Trans. Jpn Weld. Res. Inst.*, 1994, **23**, (1), 103–104.
27. M. G. Deutsch, A. Punkari, D. C. Weckman and H. W. Kerr: *Sci. Technol. Weld. Join.*, 2003, **8**, (4), 246–256.
28. A. Punkari, D. C. Weckman and H. W. Kerr: *Sci. Technol. Weld. Join.*, 2003, **8**, (4), 269–282.
29. P. F. Mendez: 'Order of magnitude scaling of complex engineering problems, and its application to high productivity arc welding', PhD thesis, Massachusetts Institute of Technology, MA, USA, 1999.
30. P. F. Mendez and T. W. Eagar: Proc. 5th Int. Conf. on 'Trends in welding research', (ed. J. M. Vitek *et al.*), 13–18; 1998, Pine Mountain, Georgia, ASM International.
31. P. F. Mendez, K. L. Niece and T. W. Eagar: Proc. Int. Conf. on 'Joining of advanced and specialty material II', (eds M. Singh, J. E. Indacocochea, K. Ikeuchi, J. Matinez, J. N. Dupont) Cincinnati, OH, USA, 1999, ASM International.
32. P. F. Mendez and T. W. Eagar: *Weld. J.*, 2003, **82**, (10), 296–306.
33. J. Biglou, 'GTA weld process modelling using principal component analysis techniques', MASc thesis, University of Waterloo, ON, Canada, 1992.
34. J. A. Brooks and J. C. Lippold: in 'ASM handbook', Vol. 6, 'Welding, brazing and soldering', (ed. J. R. Davies *et al.*), 456–457; 1993, Materials Park, OH, ASM International.
35. Lord Rayleigh: *Proc. Lond. Math. Soc.*, 1879, **10**, 4–13.
36. J. N. Anno: 'The mechanics of liquid jets'; 1977, Toronto, Lexington Books.
37. K. Ishizaki: Proc. Int. Conf. on 'Weld pool chemistry and metallurgy', London, UK, April 1980, Welding Institute, 65–76.
38. G. Simon, U. Gratzke, J. Kroos, B. Specht and M. Vicanek: Proc. ECLAT '92 Conf. on 'Laser treatment of material', Gottingen, Germany, October 1992, DGM Informationsgesellschaft mbH, 681–686.
39. H. Hügel, F. Dausinger, P. Berger, M. Beck and J. Griebsch: Proc. ECLAT '94 Conf. on 'Laser treatment of materials', Bremen,

Germany, September 1994, DVS-Verlag for Deutscher Verband fur Schweisstechnuk, 63–74.

40. U. Gratzke, P. D. Kapadia, J. Dowden, J. Kross and G. Simon: *J. Phys. D Appl. Phys.*, 1992, **25**, (11), 1640–1647.
41. C. Bagger and F. Olsen: Proc. Conf. ICALEO '98: 'Laser material processing', Orlando, FL, November 1998, Laser Institute of America, Vol. 85, 43–52.
42. F. Gao and A. Sonin: Proc. Conf. on 'Mathematical, physical and engineering sciences', 533–554; 1994, London, The Royal Society.
43. E. O. Paton, S. L. Mandel'berg and B. G. Sidorenko: *Avt. Svarka*, 1971, **24**, 1–6.
44. M. L. Lin and T. W. Eagar: *Weld. J.*, 1985, **64**, (6), 163–169.
45. M. L. Lin and T. W. Eagar: *Metall. Trans. B*, 1986, **17B**, (3), 601–607.
46. V. I. Shchetinina, L. K. Leshchinskii, A. N. Serenko, V. P. Ermolov, B. B. Sologurb, S. V. Gulakov and V. G. Bendrik: *Svar. Proiz., Weld. Produc.*, 1981, **28**, (4), 1–2.
47. M. Beck, P. Berger, F. Dausinger and H. Hügel: Proc. 8th Int. Symp. on 'Gas flow and chemical lasers', Madrid, Spain, September 1990, International Society of Optical Engineering, 769–774.
48. Y. Arata and E. Nabegata: *Trans. JWRI*, 1978, **7**, (1), 101–109.
49. K. A. Lyttle: in 'ASM handbook', Vol. 6, 'Welding, brazing and soldering', (ed. J. R. Davies *et al.*), 64 – 69; 1993, Materials Park, OH, ASM International.
50. K. Michie, S. Blackman and T. E. B. Ogunbiyi: *Weld. J.*, 1999, **78**, (5), 31–34.
51. C. Holmes: Proc. Conf. on 'Robotic arc welding', Orlando, FL, USA, December 2000, AWS, 239–255.
52. T. Ueyama, T. Ohnawa, M. Tanaka and K. Nakata: *Sci. Technol. Weld. Join.*, 2005, **10**, (6), 750–759.
53. U. Dilthey, D. Fuest, A. Huwer, J. Schneegans and L. Jacobskötter: Proc. Int. Conf. Joining/welding 2000, The Hague, Netherlands, July 1991, Pengamon Press for International Institute of Welding, 89–96.
54. J. Xie: *Weld. J.*, 2002, **81**, (10), 223–230.
55. T. Iwase, K. Shibata, H. Sakamoto, F. Dausinger, B. Hobenberger, M. Müller, A. Matsunawa and N. Seto: Proc. Conf. ICALEO 2000: 'Laser materials processing', Orlando, FL, USA, October 2000, Laser Institute of America, Vol. 89, 26–34.
56. M. Kern, P. Berger and H. Hügel: *Weld. J.*, 2000, **79**, (3), 72–78.
57. G. Shannon: 'Laser welding of sheet steel', PhD thesis, University of Liverpool, Liverpool, UK, 1993.
58. D. J. Magnusson and R. C. Threlfo: *Weld. J.*, 1969, **48**, (3), 198–203.